

## **Droplets in Two-Dimensional Ising and Potts Models**

**Walter Selke<sup>1</sup>**

*Received March 8, 1989*

---

Droplets on a wall and droplets around a nucleus in the center of the lattice are studied in the two-dimensional Ising and three-state Potts models using Monte Carlo techniques. Finite-size effects are discussed by applying a scaling argument and by relating the shape of a droplet to a random walk.

---

**KEY WORDS:** Droplets; Ising and Potts models; finite-size effects.

### **1. INTRODUCTION**

There are various ways to define droplets. Examples are freely nucleated droplets, whose equilibrium shapes follow from the Wulff construction,<sup>(1,2)</sup> and droplets on a wall.<sup>(1,3,4)</sup>

In this article finite-size effects on the shape of two types of droplets in two-dimensional Ising and three-state Potts models will be discussed. In particular, I shall consider droplets on a wall which are introduced by fixing the Ising or Potts spin variables on a segment of length  $L$  on the lower boundary of the system in a state, say,  $A$ , different from the one, say,  $B$ , on the upper and the remainder of the lower boundary. In the Ising case, exact results<sup>(1,3,5)</sup> have been obtained in the limit of  $L$  approaching infinity, for instance, on the width of the  $A$  droplet formed above the segment. The Potts case has not been considered before. Another type of droplet may be formed around a nucleus in the center of the system by fixing the variables in that center in a specific state,  $A$ , and the variables on the outer border of the system in a different state,  $B$ . The shape of the resulting  $A$  droplet will be seen to depend strongly on the size and shape of the nucleus. An apparently similar boundary condition has been con-

---

<sup>1</sup> Institut für Festkörperforschung der KFA Jülich, D-5170 Jülich, Federal Republic of Germany.

sidered recently in the context of “damage spreading”<sup>(6)</sup> in Ising models by fixing the central spin, but with no restriction on the outer border.

The outline of the article is as follows: First, I shall present results of a Monte Carlo study on droplets on a wall. These findings will be interpreted by using the concept of the random walk to describe the shape of the droplet.<sup>(3)</sup> The observed, surprisingly strong, finite-size dependences are retraced to those of the mean square step length  $b^2$  of such a walk. In Section 3, Monte Carlo results on droplets around a nucleus in the center of the lattice will be discussed. In particular, at the bulk critical temperature the radius of the droplet around the fixed central spin is found to grow with the square root of the linear dimension of the system, in accordance with a scaling argument, both in the Ising and three-state Potts cases. A short summary concludes the article.

### 2. DROPLETS ON A WALL

The geometry used to describe droplets on a wall is sketched in Fig. 1: The Ising ( $S_i = \pm 1$ ) or three-state Potts ( $S_i = 0, 1, 2$ ) variables are fixed on the boundary of a lattice of  $K_1 \cdot K_2$  spins such that  $L$  spins on a segment in the middle of the lower boundary, which is totally of length  $K_1$  (setting lattice constants equal to one), are in state  $A$  with  $A = A_I = -1$  in the Ising case and  $A = A_P = 0$  in the Potts case, while the spins on the remaining boundary are in a different state  $B$ , with  $B_I = 1$  and  $B_P = 2$ . The spins in the interior of the system interact with each other and with the ones on the boundary through the Hamiltonians

$$\mathcal{H}_1 = - \sum_{i, \delta} JS_i S_{i+\delta} \tag{1}$$

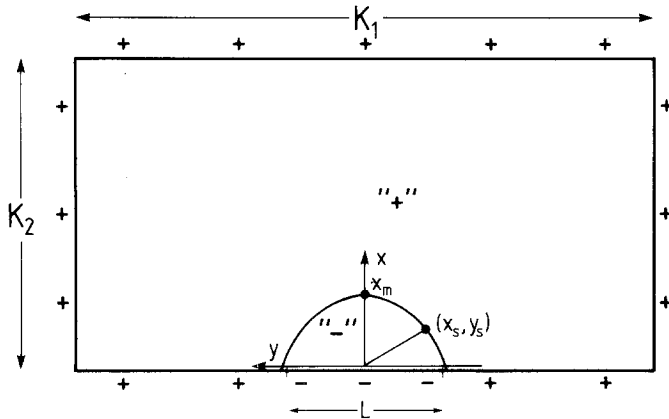


Fig. 1. Geometry of the droplet on a wall in the Ising case.

in the Ising case, where the sum runs over all lattice sites  $i$  and their neighbors,  $i + \delta$ ; and

$$\mathcal{H}_P = - \sum_{i, \delta} J \delta_{S_i, S_{i+\delta}} \tag{2}$$

in the Potts case. The coupling constant  $J$  is assumed to be positive.

Then an  $A$  droplet will be formed on the lower wall, i.e., above the segment of  $L$  spins. Its shape and size may be described by the coordinates  $(x_s, y_s)$  (see Fig. 1), with the  $y$  axis being chosen to be parallel to the lower boundary and the  $x$  axis being perpendicular to it. The origin of the coordinate system is the midpoint of the segment. At  $(x_s, y_s)$  the density of state  $A$ ,  $n_A$ , is equal to the density of state  $B$ ,  $n_B$ . In general, the density of a state, say  $C$ , with  $C_1 = \pm 1$  and  $C_P = 0, 1, 2$ ,  $n_C$ , is defined by

$$n_C(x, y) = \langle \delta_{S_{xy}, C} \rangle \tag{3}$$

where the brackets  $\langle \cdot \rangle$  denote the usual thermal average. Hence the shape of the droplet  $(x_s, y_s)$  is given by

$$n_A(x_s, y_s) = n_B(x_s, y_s) \tag{4}$$

Usually, Eq. (4) is not fulfilled for any lattice point, and one may consider densities on a continuum  $(x, y)$  by smooth interpolation between their values at the lattice sites. Examples are depicted in Figs. 2 and 3,

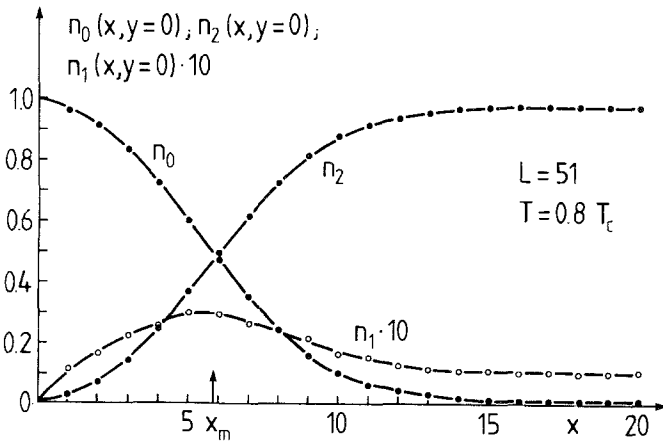


Fig. 2. Densities of state in the three-state Potts model at  $0.8T_c$  along the path  $(x, y=0)$ . The size of the system is  $131.55$ . Here  $x_m$  denotes the width of the droplet.

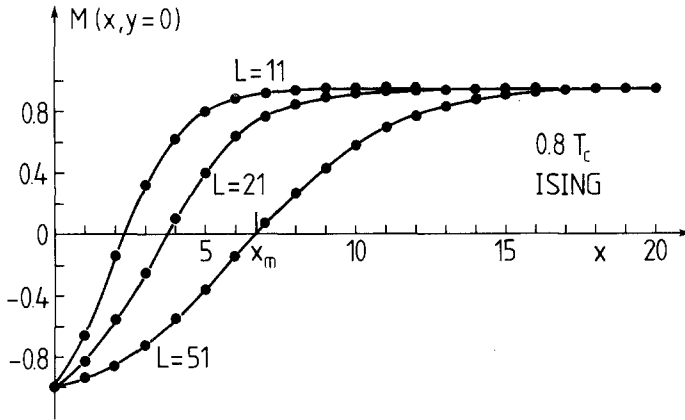


Fig. 3. Magnetization in the Ising model at  $0.8T_c$  along the path  $(x, y=0)$ . Systems of sizes  $63 \cdot 35$  ( $L=11, 21$ ) and  $121 \cdot 45$  ( $L=51$ ) are considered.

showing densities along a path perpendicular to the wall starting at the midpoint of the  $L$  segment. Of course, the droplet is expected to have its largest extent there, with the interface between the  $A$  region and the  $B$  region being at  $(x_s = x_m, y_s = 0)$ . It is interesting to note that in the Potts case the density  $n_1$  displays a maximum near that interface; see Fig. 2. Indeed, one observes the phenomenon of “interfacial adsorption,”<sup>(7)</sup> i.e., there is an excess of nonboundary states 1 at the interface separating the 0- and 2-rich regions, as has been discussed before for various multistate models.<sup>(7)</sup> This phenomenon clearly distinguishes the Potts and Ising cases. In the Ising model, (see Fig. 3) data for the magnetization  $M(x, y)$  are shown, which follows from the densities  $n_{+1}(x, y)$  and  $n_{-1}(x, y)$  by

$$M(x, y) = \langle S_{xy} \rangle = n_{+1}(x, y) - n_{-1}(x, y) \quad (5)$$

The shape of the  $-$  droplet is obtained from  $M(x_s, y_s) = 0$ .

From such smooth interpolations for the densities the entire 0 or  $-$  droplets may be mapped to study their dependence on the size of the system  $K_1$ ,  $K_2$ , and  $L$ , as well as temperature  $T$ . Illustrations are given in Figs. 4 and 5 at temperatures well below the bulk transition temperatures  $T_c$ , with  $k_B T_c(\text{Ising}) = 2J/\ln(\sqrt{2} + 1)$  and  $k_B T_c(\text{Potts}) = J/\ln(\sqrt{3} + 1)$ , namely  $T = 0.8T_c$ . At such a temperature, the correlation lengths are quite small, and finite-size effects due to the linear dimensions of the system  $K_1$  and  $K_2$  are expected to play a minor role, making it possible to study separately the influence of the length of the pinning segment,  $L$ . Of course,  $K_1$  and  $K_2$  have to be chosen to be sufficiently large compared to  $L$  and the

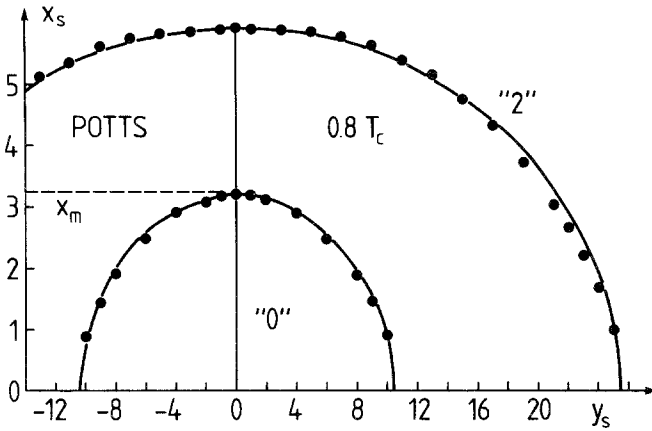


Fig. 4. Droplet shapes in the Potts model at  $0.8T_c$ . The points (●) denote Monte Carlo data, the lines are fits to the elliptical curve of Eq. (6). The sizes are  $63 \cdot 63$  ( $L = 21$ ) and  $131 \cdot 55$  ( $L = 51$ ).

width of the droplet  $x_m$ . Results on the  $L$  dependence at  $0.8T_c$  will be discussed below.

On the other hand, at the critical point  $T = T_c$ , the correlation lengths diverge, leading to possibly strong dependences of the shape and size of the droplet on  $K_1$  and  $K_2$  as well. This has been confirmed, e.g., in the Ising case for  $L = 11$  and  $K_1 = K_2 = K$  with  $K$  ranging from 11 to 101. In that range,  $x_m$  grows about linearly in  $1/K$ , and the droplet seems to approach a circular shape as  $K$  goes to infinity (see ref. 13 for details).

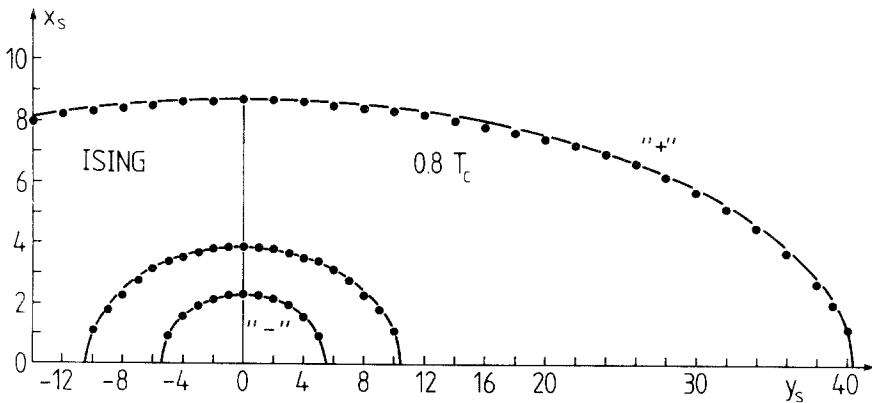


Fig. 5. Droplet shapes in the Ising model at  $0.8T_c$ . The lines and points are determined as in Fig. 4. The sizes are  $63 \cdot 35$  ( $L = 11, 21$ ) and  $121 \cdot 45$  ( $L = 81$ ).

In general, the shape of a droplet is found to be, to a very good degree of accuracy, elliptical, i.e.,

$$x_s^2 + a_1 y_s^2 = a_2 \quad (6)$$

as exemplified in Figs. 4 and 5. In those examples, and throughout the following analysis, the coefficients  $a_1$  and  $a_2$  are determined from the points  $(x_m, 0)$  and  $(x_s, y_s = \pm(L-1)/2)$ .

Very interestingly, the identification of a droplet on a wall as an ellipse follows from a description of the droplet as a random walk between the endpoints of the pinning segment  $(x_s = 0, y_s^{(+,-)})$ , as has been discussed in detail by Fisher.<sup>(3)</sup> Starting, say, at the left endpoint  $(0, y_s^{(-)})$  of the droplet, a random walk proceeds by going either forward (to the right), up, or, at later stages, down. Then, assuming the size of the droplet to be sufficiently large so that the central limit theorem can be applied for the random walk, one finds Eq. (6) with<sup>(3)</sup>

$$a_1 = 2b^2/L_0; \quad a_2 = \frac{1}{2}L_0b^2 \quad (7)$$

where  $L_0$  is the length of the wall along which the droplet is pinned,  $L_0 = y_s^{(+)} - y_s^{(-)}$ ,  $b^2$  is the mean square step length of the random walk, proceeding in the forward, down, or up direction (the backward direction would correspond to overhangs, which are not included). From Eqs. (6) and (7), the width of the droplet immediately follows,

$$x_m = \frac{b}{\sqrt{2}} L_0^{1/2} \quad (8)$$

The exponents here could have been guessed easily since the spread of a random walk of  $L_0$  steps is always of order  $bL_0^{1/2}$ . Indeed, for the Ising model, in the limit of  $L_0$  going to infinity, it has been shown rigorously<sup>(1,5)</sup> that  $x_m$  is proportional to the square root of  $L_0$ . For the Potts case, one may wonder whether the description of the droplet as a random walk still holds, in view of the phenomenon of interfacial adsorption. However, because the adsorbed state 1 interacts with the two other states 0 and 2 in the same way, one might argue that the interfacial adsorption simply renormalizes the mean square step length.

To check Eq. (8),  $x_m$  has been computed for various values of the pinning segment  $L$  at  $T = 0.8T_c$ , choosing  $K_1$  and  $K_2$  sufficiently large to be able to disregard possible additional finite-size effects, as mentioned before. Results are depicted in Fig. 6, both for the Ising and Potts cases. Obviously, for small values of  $L$ , the width of the droplet  $x_m$  increases faster than with the square root of  $L$  (the numerical differences between  $L$  and  $L_0$  are negligibly small). Actually, defining an effective exponent  $a_{\text{eff}}(L)$

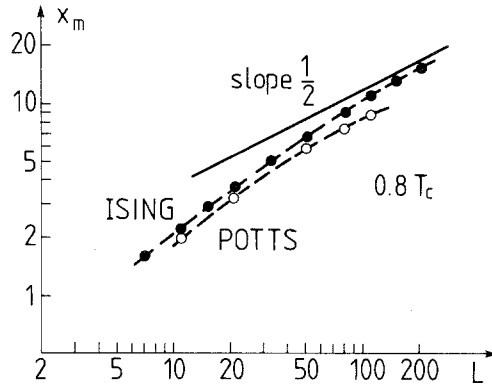


Fig. 6. The width  $x_m$  of the droplet versus the length  $L$  of the segment above which the droplet is formed, in a log-log plot for (●) Ising and (○) Potts models at  $0.8 T_c$ . The broken lines are guides to the eye; the solid line illustrates the slope  $1/2$ .

with  $a_{\text{eff}} = d(\ln x_m)/d(\ln L)$ , one finds it to decrease monotonically from a value of about  $3/4$ ,  $10 \leq L \leq 20$ , to its expected asymptotic value,  $a = 1/2$ . To approach that asymptotic value rather closely, quite large pinning segments  $L$  are needed. Roughly,  $L$  has to exceed about 110 in the Ising case, and about 70 in the Potts case at  $T = 0.8 T_c$ .

At first sight, this behavior may be rather surprising. As shown in Fig. 7, it reflects the  $L$  dependence of the mean square step length of the

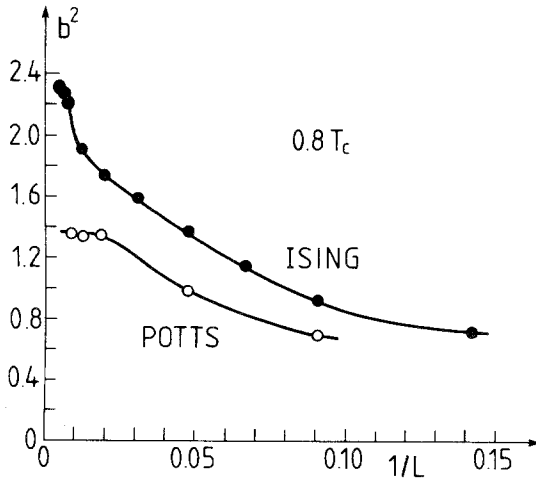


Fig. 7. The mean square step length  $b^2$  versus  $1/L$  for the (●) Ising and (○) Potts models at  $0.8 T_c$ . The solid lines are guides to the eye.

random walk. This means that Eq. (8) holds, but  $b^2$  depends strongly on  $L$ , reaching its asymptotic value only for quite large values of  $L$ . This dependence may be readily understood from the fact that the random walk is limited in its down direction, because of the wall. In other words, the droplet can fluctuate freely only toward the upper boundary, but its fluctuations are cut off by the lower boundary; see also the asymmetries in the profiles of the densities in Figs. 2 and 3. In the Potts case, such fluctuations are supposedly somewhat hindered by the interfacial adsorption of the 1 states, explaining possibly also the crossover of  $a_{\text{eff}}$  to its asymptotic value  $1/2$  at somewhat smaller values of  $L$  compared to the Ising case.

At any rate, finite-size effects are quite pronounced, and results on properties of droplets or, more generally, on interfacial phenomena close to a wall, obtained from the analysis of small lattices, such as the ones using, for instance, the transfer matrix method, have to be viewed with care (see ref. 8 for a related depinning problem).

So far, Monte Carlo results for  $T=0.8T_c$  have been presented and discussed. They are typical for temperatures below the bulk transition temperature  $T_c$ . The asymptotics are not expected to be affected by changing temperatures,  $T < T_c$ . Of course, quantities such as the width of the droplet or the mean square step length depend quantitatively on  $T$ . For instance,  $b$  has been found to increase monotonically with  $T$  at fixed  $L$ ,  $L=11$ , in the range  $0.8 \leq T/T_c \leq 1$  for the Ising case.

Certainly,  $x_m$  is expected to increase also with temperature at fixed  $L$ , which has been checked and confirmed. At  $T_c$ , the elliptical shape of the droplet seems to go over into a circular one for  $K_1=K_2=K$  approaching infinity, as mentioned before. At criticality, extremely long runs are necessary to extract reliable information, and no serious attempt has been made to investigate, e.g.,  $b(T_c, L)$ . Already at  $T=0.8T_c$ , runs of typically several  $10^4$  up to a few  $10^5$  MC steps per site are needed to get well-equilibrated data. In general, interfacial properties require very extensive simulations, due to slow relaxation and fluctuation times.<sup>(7)</sup>

Above  $T_c$ , for finite systems the definition of a droplet, Eq. (4), still holds. The width of the droplet continues to grow with temperature, but, of course, the interface between the  $A$  and the  $B$  regions becomes more and more fuzzy. No detailed simulations have been performed, because the concept of an interface loses its meaning for  $T > T_c$  in the thermodynamic limit.

### 3. DROPLETS AROUND A NUCLEUS

The boundary conditions used to generate droplets around a nucleus are sketched in Fig. 8. We consider a square lattice of  $K \cdot K$  spins. In the



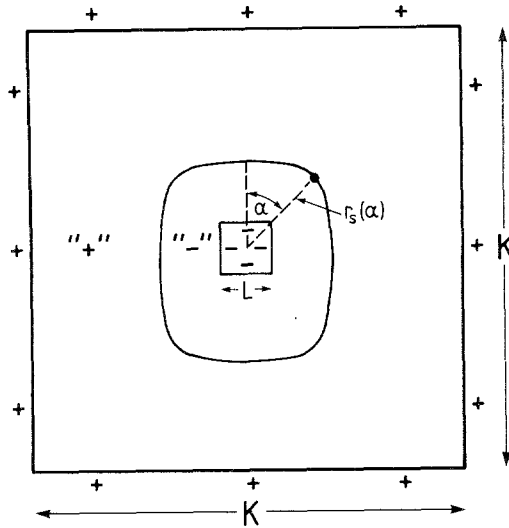


Fig. 8. Geometry of the droplet around a nucleus of  $L \cdot L$  spins in the center of the square lattice in the Ising case.

center of the lattice, the spins on a square of size  $L \cdot L$  are fixed to be in state  $A$  with  $A = A_I = -1$  in the Ising case and  $A = A_P = 0$  in the Potts case, while the spins on the outer border of the system are in a different state, with  $B_I = 1$  and  $B_P = 2$ . The interactions between the spins are described by the Hamiltonians (1) and (2).

At zero temperature, the spins outside the square in the center are in the  $B$  state. At nonzero temperatures, an  $A$  nucleus is formed around the square. Its shape and size can be determined in the same way as has been done for the nucleus on a wall; see Eq. (4). Instead of the coordinates  $(x_s, y_s)$ , one may also use radial and angular coordinates  $r_s(\alpha)$  as depicted in Fig. 8.

Using Monte Carlo techniques,  $r_s(\alpha)$  has been studied as a function of  $K$ ,  $L$ , and temperature  $T$ . At  $T < T_c$ , one observes that the shape of the droplet deviates strongly from that of a freely nucleated droplet.<sup>(2,9)</sup> The latter one follows from the interfacial tension applying the Wulff construction. It assumes an interface which can fluctuate without restrictions. However, in the case of the droplet around a nucleus, the fluctuations of the interface are always hindered by the fixed spins in the center. This restriction cannot be overcome by enlarging  $L$ , because the radius of the droplet grows more slowly than linearly in  $L$  (see the related results in the previous section). Accordingly, the shape of the droplet resembles more and more closely the shape of the center, i.e., the droplet looks more quadratic, on increasing  $L$ .

At  $T_c$ , the dependence of  $r_s(\alpha)$  on  $K$  is quite pronounced, because of the divergent correlation lengths. A detailed Monte Carlo study has been done for the case of one fixed spin in the center,  $L=1$ . The droplet takes on a circular shape, and its radius  $r$  grows continuously with  $K$ . Indeed, as shown in Fig. 9, for  $30 \leq K \leq 200$ , one finds

$$r \sim K^x \quad (9)$$

with  $x$  very close to  $1/2$ . Such an exponent follows from a scaling argument, which will be outlined in the following. Obviously, the diminishing of the  $A$  density  $n_A$  with distance  $d$  from the central spin is governed by the bulk correlation length  $\xi$ . At  $T=T_c$ , one has  $\xi \sim d^{-\eta}$ , where  $\eta = \eta_I = 1/4$  and  $\eta = \eta_P = 4/15$ ; see ref. 10. At the boundary of the droplet,  $n_A = n_B$ , the order parameter  $O$  vanishes. From standard finite-size scaling theory,<sup>(11)</sup> the size dependence of the order parameter (of course, in the  $A$  region as well as in the  $B$  region) is known to scale like  $O \sim K^{-\beta/\nu}$ , with  $\beta_I = 1/8$ ,  $\beta_P = 1/9$ ,  $\nu_I = 1$ , and  $\nu_P = 5/6$ . Therefore, one might suppose that the radius  $r$  of the droplet is given by

$$r^{-\eta} \sim K^{-\beta/\nu} \quad (10)$$

i.e., by the distance from the center at which the  $A$  density is in between the equilibrium value of the order parameter in the  $A$  and  $B$  regions. From the values for  $\eta$ ,  $\beta$ , and  $\nu$  quoted above, one immediately obtains  $x = 1/2$  in the Ising and Potts cases, in agreement with the Monte Carlo result.

As for droplets on a wall, no detailed simulations have been performed at temperatures above  $T_c$ .

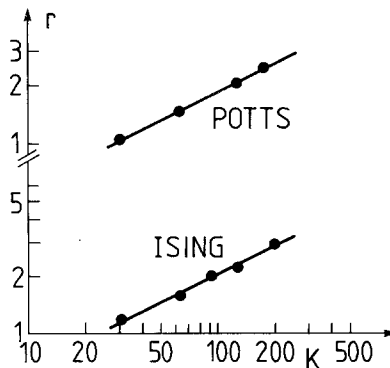


Fig. 9. Radius  $r$  of the droplet around a central spin versus the linear dimension  $K$  of the system for Ising and Potts models at  $T_c$ . The solid lines represent the slope  $1/2$ .

#### 4. SUMMARY

Using standard Monte Carlo techniques, finite-size effects of droplets have been studied in two-dimensional Ising and three-state Potts models. Pronounced finite-size effects have been observed which could be explained by relating the shape of the droplet on a wall to a random walk and by applying a scaling argument in the case of the droplet around a nucleus. In particular, the width of the droplet on a wall is expected to grow as the square root of the length of the pinning segment  $L$ . This asymptotically true behavior is masked by the pronounced  $L$  dependence of the mean square step length of the random walk describing the droplet. At criticality, the radius of the droplet around a nucleus is argued to grow with the square root of the linear dimension of the system.

The phenomenon of interfacial adsorption for the three-state Potts model is found to have only quantitative, but no qualitative consequences on the shape and size of the droplets.

Freely nucleated droplets, as encountered, for instance, in the Wulff construction, may be investigated by defining similar boundary conditions and by using, possibly, Kawasaki kinetics to conserve the number of states.

#### ACKNOWLEDGMENTS

This work originated from a discussion with J. De Coninck, which is gratefully acknowledged. It is also a pleasure to thank K. Binder for a discussion on the scaling argument, and D. Kroll, R. Lipowsky, and D. Stauffer for comments.

#### NOTE ADDED IN PROOF

The findings on the Ising droplets are confirmed by analytic results using a continuum SOS approximation<sup>(12)</sup> and conformal invariance.<sup>(13)</sup>

#### REFERENCES

1. D. B. Abraham, in *Phase Transitions and Critical Phenomena*, Vol. 10, C. Domb and J. L. Lebowitz, eds. (Academic Press, New York, 1986), p. 1.
2. H. van Beijeren and I. Nolden, in *Structure and Dynamics of Surfaces II*, W. Schommers and P. von Blanckenhagen, eds. (Springer, 1987), p. 259.
3. M. E. Fisher, *J. Stat. Phys.* **34**:667 (1984).
4. D. B. Abraham, J. De Coninck, and F. Dunlop, *Phys. Rev. B* **39**:4708 (1989).
5. D. B. Abraham, *Phys. Rev. Lett.* **44**:1165 (1980).
6. H. E. Stanley, D. Stauffer, J. Kertesz, and H. J. Herrmann, *Phys. Rev. Lett.* **59**:2326 (1987).
7. W. Selke, in *Lecture Notes in Physics*, Vol. 206, A. Pekalski and J. Sznajd, eds. (Springer, 1984), p. 191.

8. I. Schmidt and W. Pesch, *Z. Physik B* **58**:63 (1984).
9. J. E. Avron, H. van Beijeren, L. S. Schulman, and R. K. P. Zia, *J. Phys. A* **15**:L81 (1982).
10. F. Y. Wu, *Rev. Mod. Phys.* **54**:235 (1982).
11. M. N. Barber, in *Phase Transitions and Critical Phenomena*, Vol. 8, C. Domb and J. L. Lebowitz, eds. (Academic Press, New York, 1983), p. 145.
12. T. W. Burkhardt, Propagator for the Wetting Transitions in 1 + 1 Dimensions, preprint (1989).
13. T. W. Burkhardt, W. Selke and T. Xue, Droplets in the Two-Dimensional Critical Ising Model and Conformal Invariance, preprint (1989).